IOPscience iopscience.iop.org

Home Search Collections Journals About Contact us My IOPscience

Binding energies of a hydrogenic impurity and of a Wannier exciton in an arbitrary corner structure

This article has been downloaded from IOPscience. Please scroll down to see the full text article.

1996 J. Phys.: Condens. Matter 8 7443

(http://iopscience.iop.org/0953-8984/8/40/009)

View the table of contents for this issue, or go to the journal homepage for more

Download details:
IP Address: 171.66.16.207
The article was downloaded on 14/05/2010 at 04:15

Please note that terms and conditions apply.

J. Phys.: Condens. Matter **8** (1996) 7443–7451. Printed in the UK

Binding energies of a hydrogenic impurity and of a Wannier exciton in an arbitrary corner structure

Zhen-Yan Deng

China Centre of Advanced Science and Technology (World Laboratory), PO Box 8730, Beijing 100080, People's Republic of China, and
Shanghai Institute of Ceramics, Chinese Academy of Sciences, Shanghai 200050, People's Republic of China†

Received 20 December 1995, in final form 9 April 1996

Abstract. We calculate variationally the binding energies of a hydrogenic impurity and a Wannier exciton in an arbitrary corner of well material surrounded by the barrier material. The results show that the binding energy of ground impurity states in the corner can be comparable with that of highly excited impurity states in the bulk when the corner structure becomes small. However, the behaviour of the exciton in the corner is not the same as that of impurity; the binding energy of the exciton varies with the corner structure insensitively. The dependences of the impurity and exciton binding energies on the dielectric mismatch between the well material and barrier material are also discussed.

1. Introduction

Because of the importance of impurity and exciton behaviours in the future design of electronic and optical devices, studies of the hydrogenic impurity and exciton states in low-dimensional systems (quantum wells, quantum wires and quantum dots) have attracted both theoretical and experimental attention in the past few years [1–3]. Because of the confinement in the low-dimensional structures, the binding energies of impurity and exciton are enhanced considerably [4, 5]. A variational approach is an effective method for the study of impurity and exciton states in low-dimensional systems. The impurity and exciton binding energies obtained by the variational theory have been successfully compared with a variety of experimental results obtained by many researchers [2, 6–11]. Usually, step structures exist at the interfaces of low-dimensional structures [12, 13], and this affects their electronic and optical properties considerably. When the dimensions of the step structures are large enough, we can model them as corners [14]. In fact, corner structures exist in any sample, such as a semiconductor corner surrounded by vacuum or metals (metal–semiconductor heterostructures). The corner model can also be used for V-shaped grooves at the surfaces, which appeared recently in the fabrication of quantum wire structures [15–17].

In our previous paper [14], we have studied the electronic and impurity states in a right corner. However, the angle of the corner structure is not usually a right angle. A corner with an angle larger or smaller than a right angle could also exist at semiconductor interfaces

† Mailing address.

0953-8984/96/407443+09$19.50 © 1996 IOP Publishing Ltd

[18, 19] and in V-shaped grooves [15–17]. In this paper, we study the binding energies of a hydrogenic impurity and a Wannier exciton in an arbitrary corner structure. Our results indicate that the impurity binding energy decreases rapidly with decrease in the angle of the corner structure, but the exciton binding energy does not apparently change when the corner structure becomes small.

2. Electronic states

Let us consider a corner of well material of dielectric constant ϵ_1 surrounded by barrier material of dielectric constant ϵ_2, as shown in figure 1. In the effective-mass approximation, the Hamiltonian for electronic states considering the dielectric mismatch in the corner can be written

$$H^{(0)}(\boldsymbol{r}) = -\frac{\hbar^2}{2m_e}\left\{\frac{1}{\rho}\frac{\partial}{\partial\rho}\left(\rho\frac{\partial}{\partial\rho}\right) + \frac{1}{\rho^2}\frac{\partial^2}{\partial\theta^2} + \frac{\partial^2}{\partial z^2}\right\} + V_e(\boldsymbol{r}) + v_{ec}(\boldsymbol{r}) \tag{1}$$

where m_e is the electron-band effective mass, and $V_e(\boldsymbol{r})$ and $V_{ec}(\boldsymbol{r})$ are the electron image potential and the electron-confining potential in the corner, respectively. The electron-confining potential well is

$$V_{ec}(\boldsymbol{r}) = \begin{cases} 0 & |\theta| < \theta_0 \\ \infty & \text{elsewhere} \end{cases} \tag{2}$$

where $2\theta_0$ is the angle of the corner. If the electron is located at the position (ρ, θ, z) inside the corner, the electron image potential is

$$V_e(\boldsymbol{r}) = \sum_{n=1}^{m}\sum_{i=+,-}\frac{p^n e^2}{4\epsilon_1\rho|\sin[(\theta-\theta_n^i)/2]|} \tag{3}$$

where

$$p = \frac{\epsilon_1 - \epsilon_2}{\epsilon_1 + \epsilon_2}$$

and (ρ, θ_n^i, z) is the position of the electron image charge

$$\theta_n^{\pm} = \begin{cases} \theta \pm 2n\theta_0 \\ -\theta \pm 2n\theta_0 \end{cases} \qquad \text{for} \begin{cases} \text{even } n \\ \text{odd } n \end{cases} \tag{4}$$

with $n = 1, 2, \ldots, m$ and

$$|\theta_{m-1}^{\pm} \pm \theta_0| < \pi. \tag{5}$$

In the case when $p \geqslant 0$, i.e. $\epsilon_1 \geqslant \epsilon_2$, which corresponds to the situation of a semiconductor corner surrounded by vacuum or other materials with smaller dielectric constants, the electron image potential inside the corner is positive (this can be seen from equation (3)), and no localized electronic states exist in the corner. As the simplest approximation, the electronic wavefunctions in the corner that we adopted are the same as those which do not include the dielectric mismatch (see the appendix). The ground level and electronic wavefunctions are

$$\begin{aligned} &E_0 = 0 \\ &\Phi_0(\boldsymbol{r}) = 0. \end{aligned} \tag{6}$$

In the case when $p < 0$, i.e. $\epsilon_1 < \epsilon_2$, which is the situation of semiconductor or vacuum corners surrounded by metals [20], the electron image potential inside the corner is

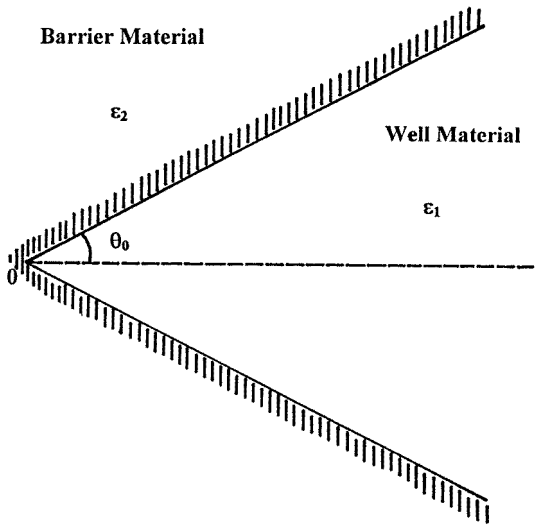

Figure 1. The schematic representation of the corner structure that we considered, where the well material and barrier material are inside the corner and outside the corner, respectively.

negative, and localized electronic states exist in the corner. According to the discussion in the appendix, the following trial wavefunction for the ground electronic state in the corner is used:

$$\Phi_0(\boldsymbol{r}) = N_0 \rho^{\nu} \cos(\nu\theta) \exp\left(-\frac{\rho}{\alpha}\right) \qquad \left(\nu = \frac{\pi}{2\theta_0}\right) \tag{7}$$

where N_0 is the normalization constant and α is the variational parameter. The wavefunction (7) satisfies the boundary condition. The ground electronic level is obtained as follows:

$$E_0 = \min_{\alpha} \langle \Phi_0(\boldsymbol{r}) | H^{(0)}(\boldsymbol{r}) | \Phi_0(\boldsymbol{r}) \rangle. \tag{8}$$

3. Impurity and exciton states

When a hydrogenic impurity is placed at the position $(\rho_1, \theta_1, 0)$ inside the corner, the Hamiltonian for the impurity states can be written

$$H^{(1)}(\boldsymbol{r}) = -\frac{\hbar^2}{2m_e}\left\{\frac{1}{\rho}\frac{\partial}{\partial\rho}\left(\rho\frac{\partial}{\partial\rho}\right) + \frac{1}{\rho^2}\frac{\partial^2}{\partial\theta^2} + \frac{\partial^2}{\partial z^2}\right\} + V_{ion}(\boldsymbol{r}) + V_e(\boldsymbol{r}) + V_{ec}(\boldsymbol{r}) \tag{9}$$

where

$$V_{ion}(\boldsymbol{r}) = -\sum_{n=0}^{m}\sum_{i=+,-} \frac{p^n e^2}{\epsilon_1[\rho^2 + \rho_I^2 - 2\rho\rho_I \cos(\theta - \theta_{In}^i) + z^2]^{1/2}} \tag{10}$$

is the sum of the impurity ion potential and its image potentials inside the corner. The position of the impurity ion image charge $(\rho_I, \theta_{In}^i, 0)$ is the same as that of the electron image charge (equation (4)) if only θ is replaced by θ_I.

If the centre-of-mass motion in the z direction is omitted, the Hamiltonian for a Wannier exciton in the corner is given in the effective-mass approximation as

$$H^{(2)}(\boldsymbol{r}) = -\frac{\hbar^2}{2m_e}\left\{\frac{1}{\rho_e}\frac{\partial}{\partial\rho_e}\left(\rho_e\frac{\partial}{\partial\rho_e}\right)+\frac{1}{\rho_e^2}\frac{\partial^2}{\partial\theta_e^2}\right\}-\frac{\hbar^2}{2m_h}\left\{\frac{1}{\rho_h}\frac{\partial}{\partial\rho_h}\left(\rho_h\frac{\partial}{\partial\rho_h}\right)+\frac{1}{\rho_h^2}\frac{\partial^2}{\partial\theta_h^2}\right\}$$
$$-\frac{\hbar^2}{2\mu}\frac{\partial^2}{\partial z^2}-\frac{e^2}{\epsilon_1[\rho_e^2+\rho_h^2-2\rho_e\rho_h\cos(\theta_e-\theta_h)+z^2]^{1/2}}+V_e(\boldsymbol{r})$$
$$+V_h(\boldsymbol{r})+V_{e-h}(\boldsymbol{r})+V_{h-e}(\boldsymbol{r})+V_{ec}(\boldsymbol{r})+V_{hc}(\boldsymbol{r}) \tag{11}$$

where m_h is the hole-band effective mass, $\mu = m_e m_h/(m_e+m_h)$ is the reduced electron–hole mass, $V_h(\boldsymbol{r})$ is the hole image potential, $V_{hc}(\boldsymbol{r})$ is the hole-confining potential in the corner, and $V_{e-h}(\boldsymbol{r})$ and $V_{h-e}(\boldsymbol{r})$ are the interaction potentials between the electron and hole image charges and between the hole and electron image charges, respectively:

$$V_h(\boldsymbol{r}) = \sum_{n=1}^{m}\sum_{i=+,-}\frac{p^n e^2}{4\epsilon_1\rho_h|\sin[(\theta_h-\theta_{hn}^i)/2]|} \tag{12}$$

$$V_{hc}(\boldsymbol{r}) = \begin{cases} 0 & |\theta_h| < \theta_0 \\ \infty & \text{elsewhere} \end{cases} \tag{13}$$

$$V_{e-h}(\boldsymbol{r}) = -\sum_{n=1}^{m}\sum_{i=+,-}\frac{p^n e^2}{\epsilon_1[\rho_e^2+\rho_h^2-2\rho_e\rho_h\cos(\theta_e-\theta_{hn}^i)+z^2]^{1/2}} \tag{14}$$

$$V_{h-e}(\boldsymbol{r}) = -\sum_{n=1}^{m}\sum_{i=+,-}\frac{p^n e^2}{\epsilon_1[\rho_h^2+\rho_e^2-2\rho_h\rho_e\cos(\theta_h-\theta_{en}^i)+z^2]^{1/2}}. \tag{15}$$

Also, the position $(\rho_h, \theta_{hn}^i, 0)$ of the hole image charge is the same as that of electron image charge if only θ is replaced by θ_h.

The trial wavefunctions for ground impurity and exciton states, we take to be written [5, 14]

$$\psi_1(\boldsymbol{r}) = N_1\rho^\nu\cos(\nu\theta)\times\exp\left(-\frac{[\rho^2+\rho_I^2-2\rho\rho_I\cos(\theta-\theta_I)+z^2]^{1/2}}{\beta}\right)\qquad\left(\nu=\frac{\pi}{2\theta_0}\right) \tag{16}$$

and

$$\psi_2(\boldsymbol{r}) = N_2\rho_e^\nu\cos(\nu\theta_e)\rho_h^\nu\cos(\nu\theta_h)\times\exp\left(-\frac{[\rho_e^2+\rho_h^2-2\rho_e\rho_h\cos(\theta_e-\theta_h)+z^2]^{1/2}}{\lambda}\right)\qquad\left(\nu=\frac{\pi}{2\theta_0}\right) \tag{17}$$

where N_1 and N_2 are the normalization constants, and β and λ are the variational parameters. The impurity and exciton binding energies in the corner are obtained as follows:

$$E_i = E_0 - \min_{\beta}\langle\psi_1(\boldsymbol{r})|H^{(1)}(\boldsymbol{r})|\psi_1(\boldsymbol{r})\rangle \tag{18}$$

$$E_{e-h} = E_0^e + E_0^h - \min_{\lambda}\langle\psi_2(\boldsymbol{r})|H^{(2)}(\boldsymbol{r})|\psi_2(\boldsymbol{r})\rangle \tag{19}$$

where $E_0^e(E_0^h)$ is the ground electronic (hole) level in the corner, which has been obtained in section 2. The above integrals were calculated numerically.

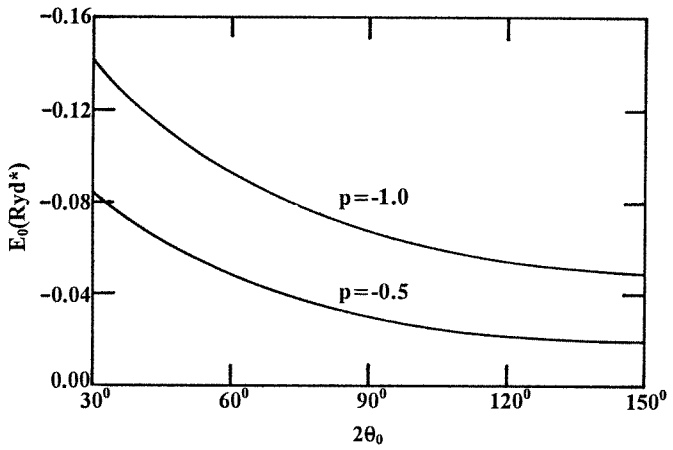

Figure 2. The dependence of the ground-state electronic level on the angle of the corner structure for two different dielectric mismatches.

4. Results and discussion

Figure 2 shows the dependence of the ground-state energy level for localized electronic states on the angle of the corner structure, where the energy is in units of effective Rydbergs: $\mathrm{Ryd}^* = m_e e^4/2\overline{h}^2\epsilon_1^2$. In figure 2, we can see that the ground-state energy level increases with decrease in the angle of corner structure and, the larger the dielectric mismatch p, the larger the ground-state electronic level is (absolute value). The situation considered in figure 2 could correspond to practical corner structures, for instance semiconductor or vacuum corners surrounded by metals ($p \simeq -1$) [20]. In fact, the image states on the metal surfaces have been detected by photoelectron spectra [21]. It is expected that localized image states in the vacuum or semiconductor corners surrounded by metals could be detected more easily because of the deeper ground level in the corners than on the surfaces, as shown in figure 2.

Figure 3 shows the dependence of the impurity binding energy on the angle of corner structure, where the impurity is placed inside the corner. From figure 3, it is apparent that, different from the behaviours of impurity states in the quantum wells and quantum wires, the impurity binding energy in the corner decreases with decrease in the angle of corner. The results in figure 3 also indicate that the impurity binding energy in the corner can be comparable with that of highly excited impurity states in the bulk when the corner structure is small. Also, the larger the dielectric mismatch (from negative to positive), the larger the impurity binding energy is. In our calculation, the following parameters are used: the electron-band effective mass $m_e = 0.067m_0$ for GaAs, and the static dielectric constants $\epsilon_1 = 13.1\epsilon_0$ and $\epsilon_2 = 10.1\epsilon_0$ for GaAs and AlAs, respectively [4], where m_0 and ϵ_0 are the free-electron mass and the vacuum static dielectric constant, respectively. Because the dielectric mismatch in the vacuum/GaAs corner is larger than that in the AlAs/GaAs corner, the corresponding impurity binding energy in the vacuum/GaAs corner is larger than that in the AlAs/GaAs corner, as shown in figure 3(b).

Figure 4 shows the dependence of the exciton binding energy on the angle of the corner structure, where we have used the effective Rydberg $\mathrm{Ryd}^* = \mu e^4/2\overline{h}^2\epsilon_1^2$ as the unit of energy with the hole-band effective mass $m_h = 5.0m_e$ in the calculation of figure 4(a). In

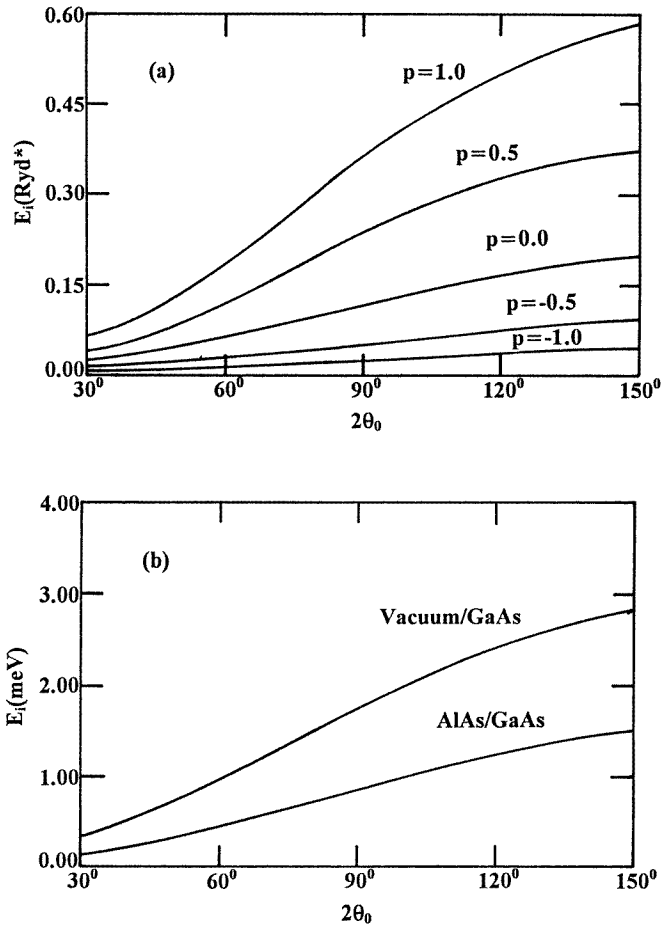

Figure 3. The dependence of the impurity binding energy on the angle of the corner structure with (a) five different dielectric mismatches and (b) well material GaAs and barrier materials AlAs and vacuum, where the impurity is located at the position $(\rho_I, 0, 0)$ where $\rho_I = 0.05a_0^*$ and $a_0^* = \hbar^2\epsilon_1/m_e e^2$ is the effective Bohr radius.

figure 4(b), the heavy-hole and light-hole effective masses for GaAs are $m_{hh} = 0.35m_0$ and $m_{lh} = 0.08m_0$, respectively [22]. From figure 4, we can see that the variations in exciton binding energy with the angle of corner structure are not as rapid as those in the impurity binding energy, i.e. the exciton binding energy varies with the corner structure insensitively. Also, the larger the dielectric mismatch (from negative to positive), the larger the exciton binding energy is, and the corresponding exciton binding energy in the vacuum/GaAs corner is larger than that in the AlAs/GaAs corner.

The above results are interesting and their physical interpretation is as follows. Because of the confinement of the electron in the corner structure, the barrier pushes the electron from the impurity ion in the corner, and the probability that an electron appears in the vicinity of impurity ion is smaller than that in the bulk; so the impurity binding energy in the corner structure is much smaller than that in the bulk [14]. When the angle of the corner structure is small, the probability that an electron appears in the vicinity of an impurity ion

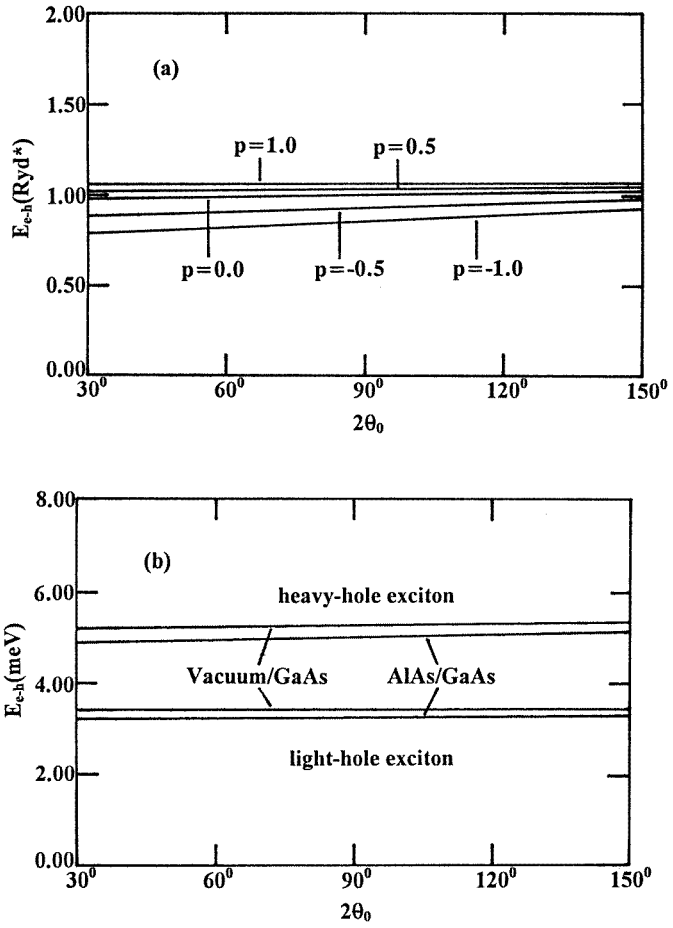

Figure 4. The dependence of exciton binding energy on the angle of the corner structure with (a) five different dielectric mismatches and (b) well material GaAs and barrier materials AlAs and vacuum.

is small. This is the reason why the impurity binding energy decreases with decrease in the angle of the corner structure. At the same time, we note that the electron wavefunctions for impurity states in the corner are similar to those of highly excited impurity states in the bulk when the angle of the corner structure is small. For instance, when the dielectric mismatch between the well material and barrier material is omitted and the corner structure angle $2\theta_0 = 90^\circ, 60^\circ, \ldots, 30^\circ$, the electron wavefunctions for impurity states in the corner are analogous to those of third, fourth, ..., seventh impurity excited states in the bulk which have been shown in equation (16), and the corresponding impurity binding energies in the corner are in the vicinity of $\frac{1}{9}, \frac{1}{16}, \ldots, \frac{1}{49}$Ryd*, as shown in figure 3(a). However, the wavefunctions for exciton states in the corner are not the same as those of the impurity states, because the centre of mass of the exciton can exist everywhere in the corner, and the effects of the barrier of the corner structure on the wavefunctions of exciton states are not as large as those of impurity states; so the exciton binding energy varies with the corner structure insensitively. When the dielectric mismatch p changes from negative to positive, the impurity ion image potentials change from positive to negative, as shown in

equation (10). Because the impurity ion potential is negative, the impurity binding energy increases with increase in the dielectric mismatch [14]. This also happens in the situation when there are exciton states in the corner structure.

In summary, we have studied impurity and exciton states in an arbitrary corner structure. Our results indicate that the impurity binding energy decreases with decrease in the angle of the corner structure, but the exciton binding energy does not apparently change when the angle of the corner structure becomes small. Step structures with large sizes and practical corner structures usually appear in low-dimensional systems as mentioned above. We believe that our results are helpful in the understanding of the electronic and optical properties of the doped low-dimensional structures with large steps or corners.

Appendix

When the dielectric mismatch between the well material and barrier material is neglected, the eigenvalue equation for the Hamiltonian $H^{(0)}(\boldsymbol{r})$ is

$$-\frac{\hbar^2}{2m_e}\left\{\frac{1}{\rho}\frac{\partial}{\partial\rho}\left(\rho\frac{\partial}{\partial\rho}\right)+\frac{1}{\rho^2}\frac{\partial^2}{\partial\theta^2}+\frac{\partial^2}{\partial z^2}\right\}\Phi(\boldsymbol{r})=E\Phi(\boldsymbol{r}). \tag{A1}$$

If we assume that the eigenfunction for $H^{(0)}(\boldsymbol{r})$ can be written

$$\Phi(\boldsymbol{r})=R(\rho)\varphi(\theta)\phi(z) \tag{A2}$$

then equation (A1) can be divided into three independent equations which can be solved easily, i.e.

$$\frac{1}{\rho}\frac{\partial}{\partial\rho}\left(\rho\frac{\partial R}{\partial\rho}\right)+\left(k_\perp^2-\frac{\nu^2}{\rho^2}\right)R=0 \tag{A3a}$$

$$\frac{\partial^2\varphi}{\partial\theta^2}+\nu^2\varphi=0 \tag{A3b}$$

$$\frac{\partial^2\phi}{\partial z^2}+k_z^2\phi=0 \tag{A3c}$$

where

$$k_\perp^2+k_z^2=\frac{2m_e}{\hbar^2}E. \tag{A4}$$

The solution of equation (A3a) is a Bessel function, and the wavefunction in the z direction is a plane wave:

$$R(\rho)=J_\nu(k_\perp\rho) \tag{A5a}$$

$$\phi(z)=L^{1/2}\exp(\mathrm{i}k_z z) \tag{A5b}$$

where L is the length of the system in the z direction. By the boundary condition of the electron wavefunction in the corner, namely

$$\varphi(\theta)|_{\theta=\pm\theta_0}=0 \tag{A6}$$

the eigenfunction of equation (A3b) is obtained as follows:

$$\varphi(\theta)=\begin{cases}\theta_0^{1/2}\cos(\nu\theta)\\ \theta_0^{1/2}\sin(\nu\theta)\end{cases}\qquad\text{for}\begin{cases}\nu=(n+\frac{1}{2})\pi/\theta_0 & (n=0,1,2,\ldots)\\ \nu=n\pi/\theta_0 & (n=1,2,\ldots)\end{cases} \tag{A7}$$

where $\nu > 0$, because the electron wavefunction should be finite when ρ tends to zero, as seen from equation (A5*a*). The ground level and wavefunction of the system are

$$E_0 = 0 \qquad \Phi_0(\boldsymbol{r}) = 0. \tag{A8}$$

References

[1] Liu X, Petrou A, McCombe B D, Ralston J and Wicks G 1988 *Phys. Rev.* B **38** 8522
[2] Simmonds P E, Birkett M J, Skolnick M S, Tagg W I E, Sobkowicz P, Smith G W and Whittaker D M 1994 *Phys. Rev.* B **50** 11 251
[3] Adelabu J S A 1995 *Physica* B **205** 65
[4] Mailhiot C, Chang Y C and McGill T C 1982 *Phys. Rev.* B **26** 4449
[5] Feng Y P and Spector H N 1993 *Phys. Rev.* B **48** 1963
[6] Oliveira L E and Falicov L M 1986 *Phys. Rev.* B **34** 8687
[7] Fraizzoli S, Bassani F and Buczko R 1990 *Phys. Rev.* B **41** 5096
[8] Barmby P W, Dunn J L and Bates C A 1994 *J. Phys.: Condens. Matter* **6** 751
[9] Carneiro G N, Weber G and Oliveira L E 1995 *Semicond. Sci. Technol.* **10** 41
[10] Latgé A, Porras-Montenegro N and Oliveira L E 1995 *Phys. Rev.* B **51** 2259
[11] Arulmozhi M and Balasubramanian S 1995 *Phys. Rev.* B **51** 2592
[12] Vecek K, Sawada A and Usagawa T 1994 *Appl. Phys. Lett.* **65** 3096
[13] Kiselev A A and Rössler U 1994 *Phys. Rev.* B **50** 14 283
[14] Deng Z Y, Zhang H and Guo J K 1994 *J. Phys.: Condens. Matter* **6** 9729, and references therein
[15] Kapon E, Kash K, Clausen E M, Hwang D M and Colas E 1992 *Appl. Phys. Lett.* **60** 477
[16] Nagamune Y, Arakawa Y, Tsukamoto S, Nishioka M, Sasaki S and Miura N 1992 *Phys. Rev. Lett.* **69** 2963
[17] Tsukamoto S, Nagamune Y, Nishioka M and Arakawa Y 1993 *Appl. Phys. Lett.* **62** 49
[18] Tolan M, Press W, Brinkop F and Kotthaus J P 1995 *Phys. Rev.* B **51** 2239
[19] Leadbeater M L, Foden C L, Burroughes J H, Pepper M, Burke T M, Wang L L, Grimshaw M P, Ritchie D A 1995 *Phys. Rev.* B **52** R8629
[20] Babiker M 1993 *J. Phys.: Condens. Matter* **5** 2137
[21] Fischer R and Fauster T 1995 *Phys. Rev.* B **51** 7112
[22] Cen J, Chen R and Bajaj K K 1994 *Phys. Rev.* B **50** 10 947